RSC Advances

Thorough investigation of varying template combinations on SAPO-34 synthesis and catalytic activity and stability in the methanol conversion to light olefin

Journal:	*RSC Advances*
Manuscript ID:	RA-ART-08-2014-008607.R1
Article Type:	Paper
Date Submitted by the Author:	10-Sep-2014
Complete List of Authors:	Sedighi, Mehdi; Tarbiat Modares University, Towfighi, Jafar; tarbiat modares university, Chemical engineering Bahrami, Hussein; tarbiat modares university, Chemical engineering

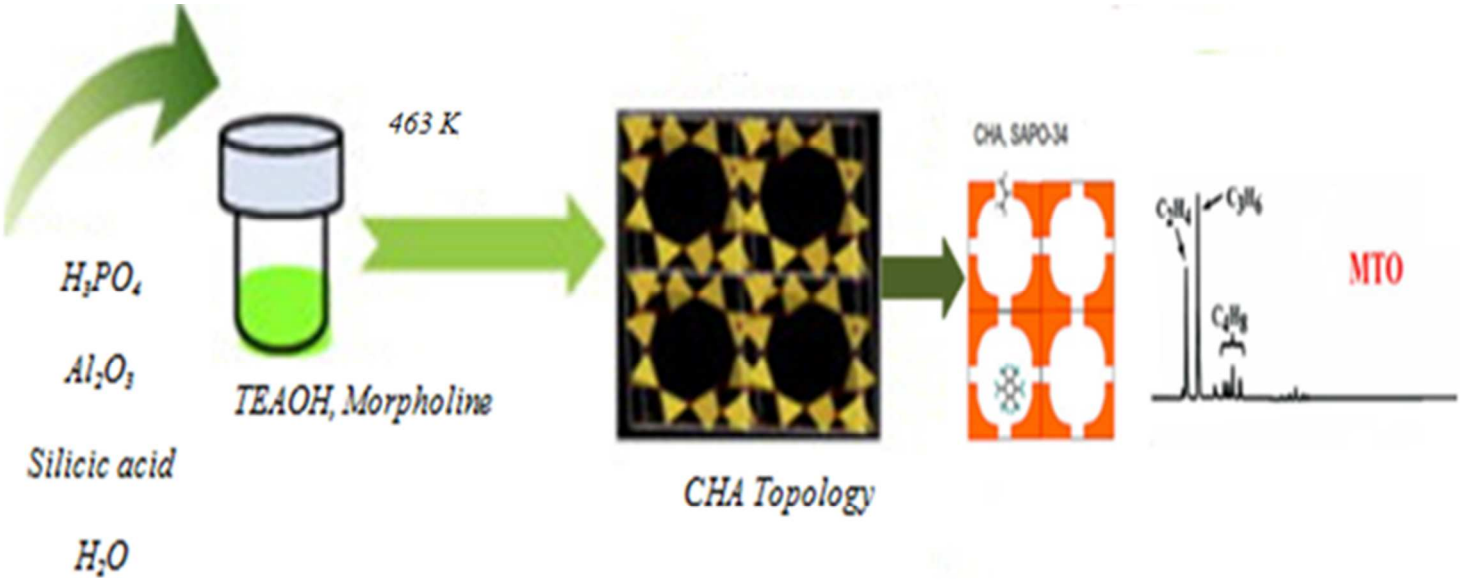
H_3PO_4
Al_2O_3
Silicic acid
H_2O
463 K
TEAOH, Morpholine
CHA Topology
CHA, SAPO-34
MTO

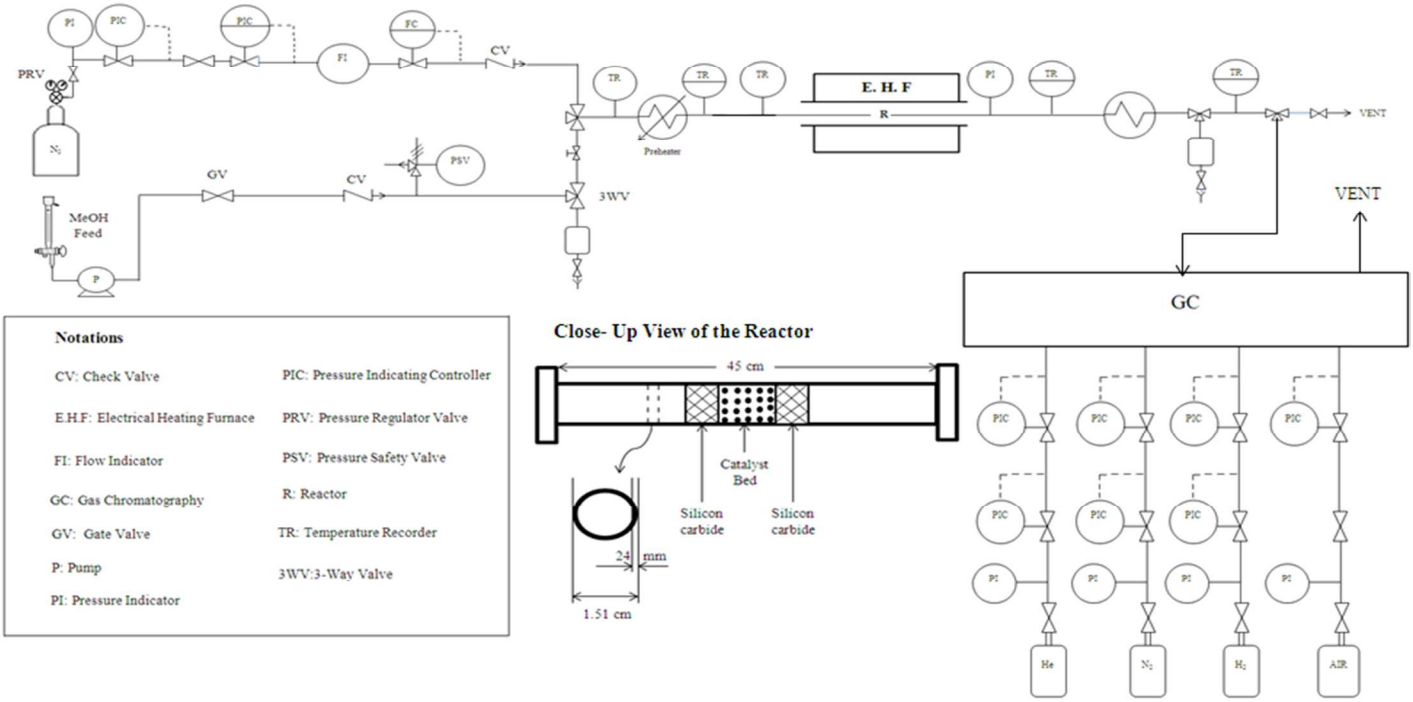

Figure1. Experimental fixed-bed setup for the MTO process

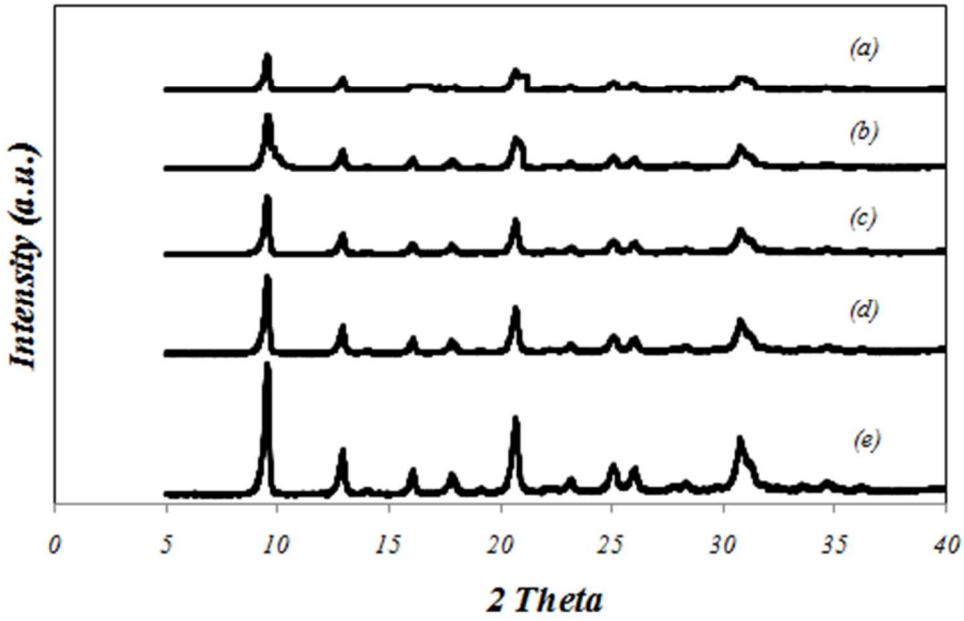

Figure2. XRD patterns of as-synthesized samples: (a) X=0, (b) X=0.41, (c) X=1, (d) X=1.59, (e) X=2.

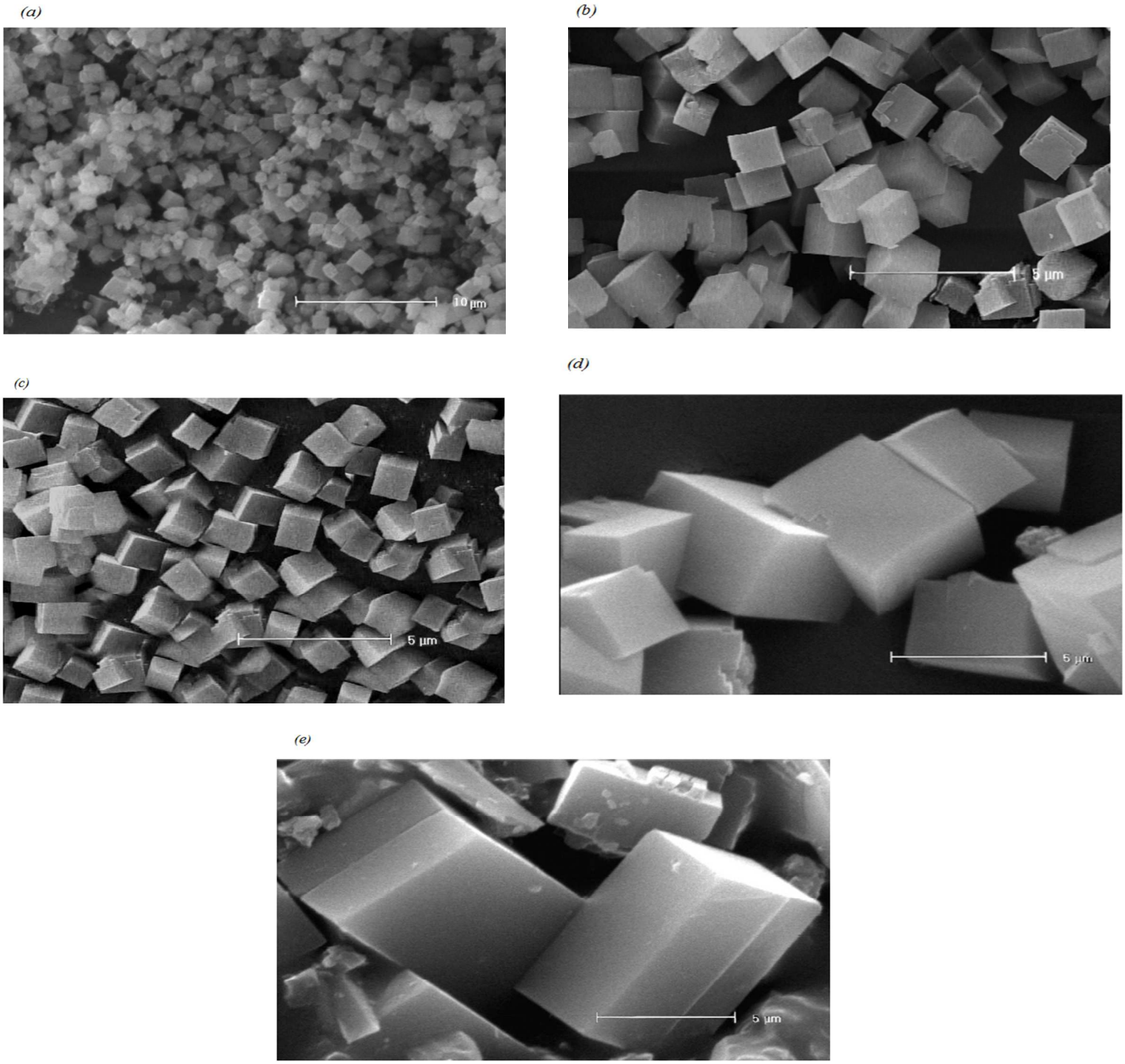

Figure3. SEM images of the prepared SAPO samples: (a) X=0, (b) X=0.41, (c) X=1, (d) X=1.59, (e) X=2.

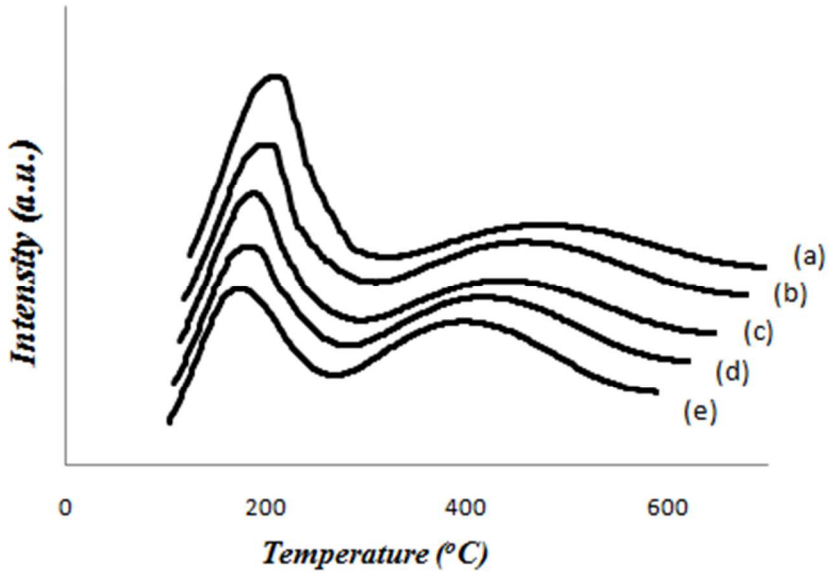

Figure4. NH_3-TPD profiles for the calcined SAPO-34 catalysts: (a) X=0, (b) X=0.41, (c) X=1, (d) X=1.59, (e) X=2.

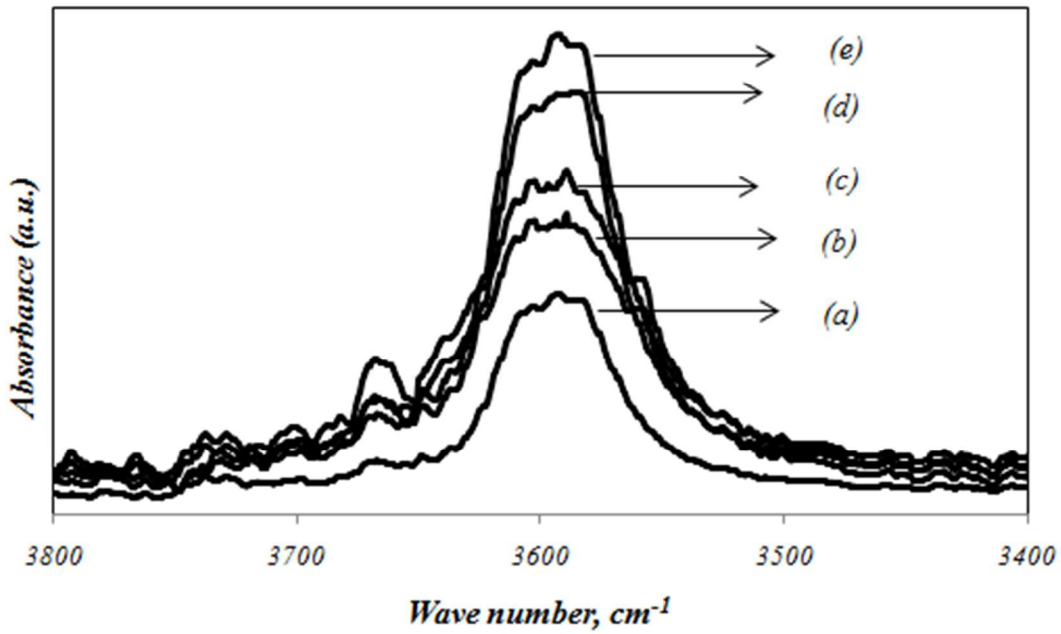

Figure5. In situ Fourier transform IR spectra of SAPO-34 in the OH stretching vibration (a) X=0, (b) X=0.41, (c) X=1, (d) X=1.59, (e) X=2.

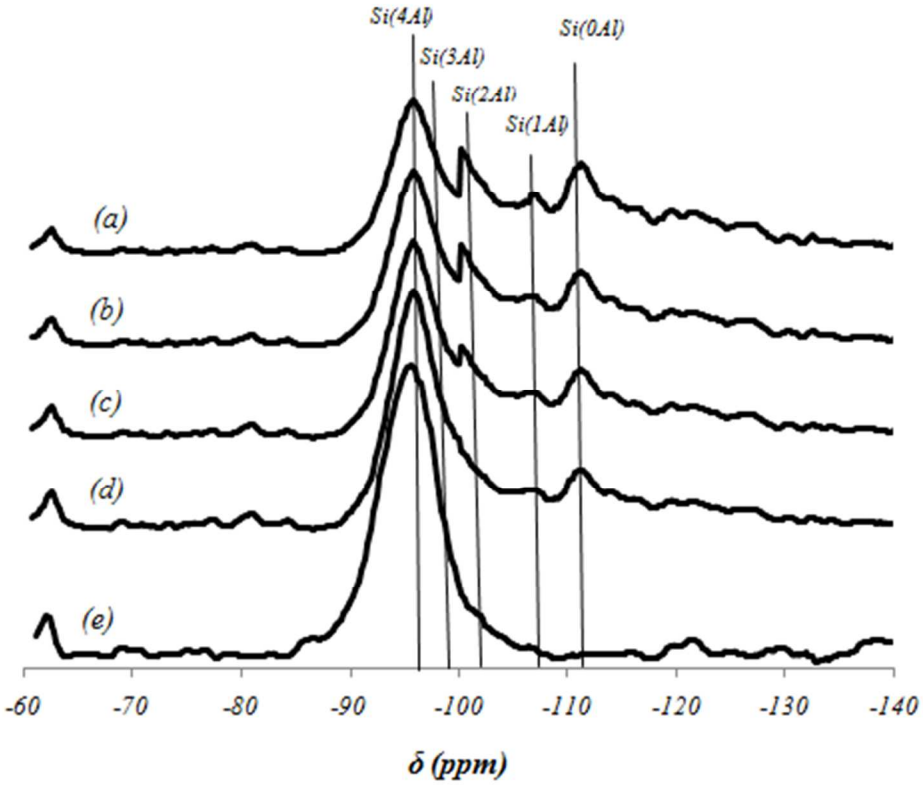

Figure6. ^{29}Si MAS NMR spectra of the calcined samples: (a) X=0, (b) X=0.41, (c) X=1, (d) X=1.59, (e) X=2

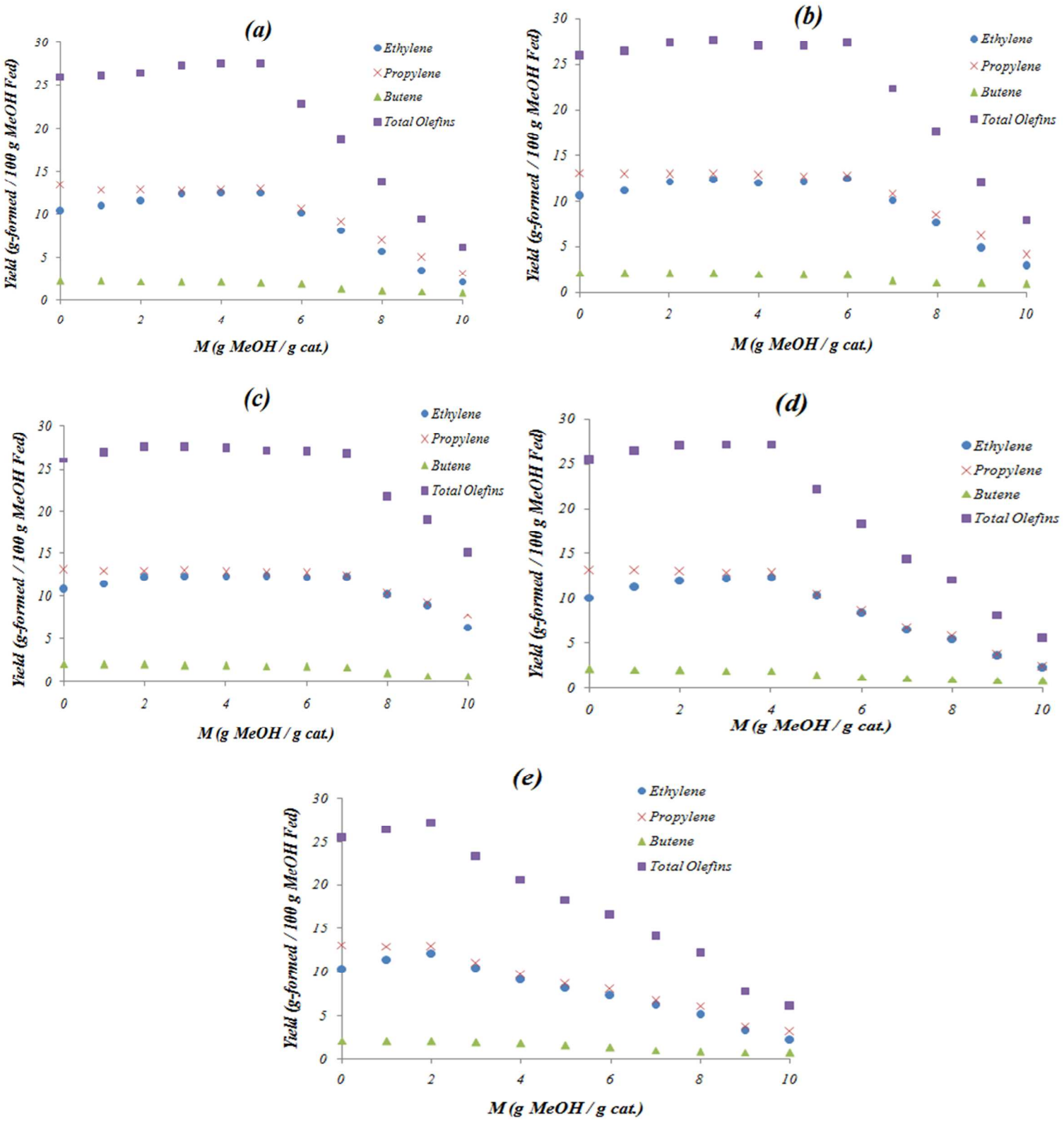

Figure7. Yields of ethylene, propylene, butene and C_2-C_4 olefins with run length over SAPO-34 catalysts. (a)X=0, (b) X=0.41, (c) X=1, (d) X=1.59, (e) X=2. Feed: 20mol% methanol with 80mol% water, Temperature: 425 °C, $W/F^0_{MeOH} = 9\ g_{cat}.hr/mol.$

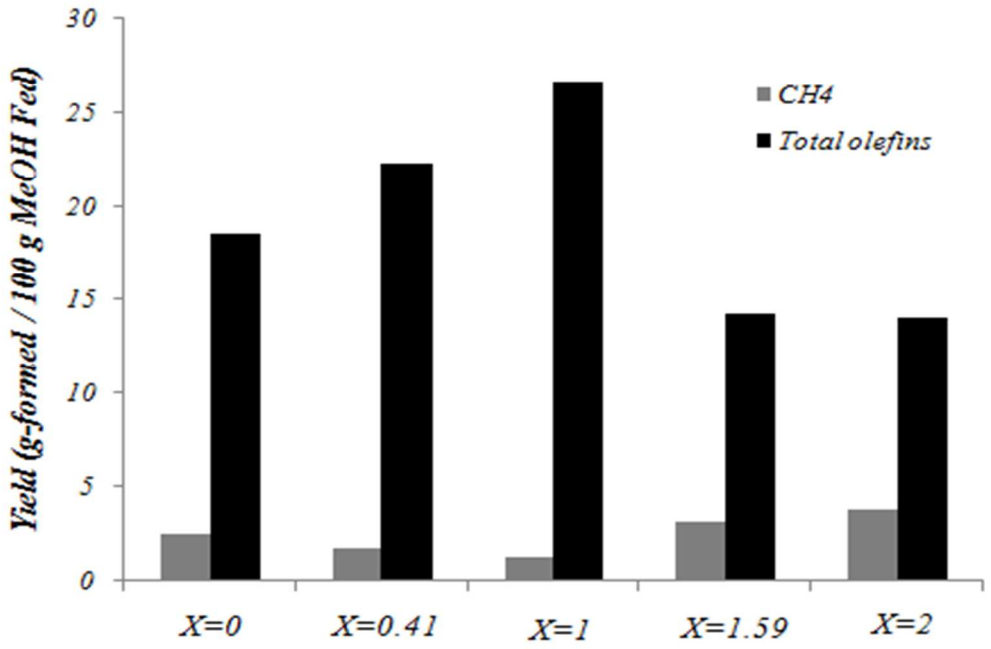

Figure8. Yields of methane and total olefins During MTO reaction over five different SAPO-34 catalysts after 120 min on stream (M ≈ 7)

Thorough investigation of varying template combinations on SAPO-34 synthesis and catalytic activity and stability in the methanol conversion to light olefin

Mehdi Sedighi, Hussein Bahrami, Jafar Towfigh Darian[*]

Department of Chemical Engineering, Tarbiat Modares University, P.O.Box14115 143, Tehran, Iran

Abstract- Crystals of SAPO-34 molecular sieves were synthesized under hydrothermal conditions by using tetraethylammonium hydroxide, morpholine and a mixture of them as structure-directing agents. The properties of the catalysts were characterized using XRD, SEM, BET, ICP, FT-IR, ^{29}Si MAS NMR and NH_3-TPD. Characterization studies showed that using a mixed template lead to the reduction of particle size and increase in external surface area. The catalytic performance of the synthesized catalysts was tested in MTO reaction with different time-on-stream. All the samples showed high activity and selectivity to light olefins at the initial stage of the reaction. The maximum yield of ethylene, propylene and butene was determined 12.57, 13.45 and 2.21 wt.%, respectively. The catalyst produced by the tetraethylammonium hydroxide /morpholine ratio of 1:1 exhibited the longest catalyst lifetime.

Keywords: MTO; SAPO-34; Acidity; Crystallite size, Stability

[*] **Corresponding Author**; Telephone: +98(21)(82883311). Email: towfighi@modares.ac.ir and/or sedighi.ac@gmail.com

1. Introduction

Light olefins, ethylene and propylene, are basic feedstocks for the petrochemical industries. The worldwide demand and production of olefins are relatively higher than for any other chemicals [1-3]. Many attempts have been taken away to produce light olefins from other non-petroleum resources due to crude oil shortage and prices. Methanol-to-olefins (MTO) conversion is a novel process for the production of light olefins from alternative and abundant resources of natural gas or coal[4]. This reaction is effectively catalyzed by various zeolites and zeotype molecular sieves. ZSM-5 was the first to be applied-producing a range of hydrocarbons especially aromatics and paraffins[5-7].

Lately, the role of molecular sieves (SAPOs) has been studied, with special attention on SAPO-34, which allows the production of a higher propotion of C_2-C_4 olefins. Attempts for controlling the selectivity of the main olefin products of methanol conversion through modification of the physico-chemical properties of SAPO-34 catalyst is continuing. The adjustment of acidity as well as shape selectivity to promote product selectivity and/or control deactivation behavior are two key attributes that help researchers modify the reactor performance of such acidic crystalline material [8, 9].

Different factors affect the acidity and morphology of microporous silicoaluminophosphate. Several studies investigated the effects of silicon and aluminum precursors [10,11], phosphorus and water contents[12, 13], and silicon amounts[14-17] on the particle size, morphology and the number of acid sites.

In forming the reaction mixture from which the silicoaluminophosphates are crystallized the organic templating agent can take on an important part. It performs structure-directing, charge-compensating, and space-filling role [18,19]. Therefore, the physico-chemical properties and

thereby the catalytic performance of solid material could be altered with the utilization of different templates. Wang et al.[20] examined the effects of a template concentration and crystallization time on the physicochemical properties and catalytic performance of SAPO-34 using triethyl amine as a template. The crystallinity and morphology of SAPO-34 were influenced by the concentration of the template. Pure SAPO-34 was obtained when the TEA/Al_2O_3 molar ratio was higher than 2.0.

Muñoz et al.[21] investigated the effects of different templates such as triethyl amine, TEAOH, morpholine on the synthesis of SAPO-34. Although materials with the same framework structure were obtained in all cases, they possessed different physicochemical properties, especially textural parameters and crystal size. Their data showed an important influence of the external surface, crystal size and acidity on the activity, selectivity and lifetime of the different samples. The sample synthesized with TEAOH as structure directing agent rendered the best catalytic performance owing to its higher external surface, smaller crystal size and higher acidity. Wilson and Barger [22] considered the synthesis of SAPO-34 with TEAOH and determined the influence by the different characteristics which affect the catalytic performance in the MTO process, i.e. shape selectivity, acid site strength, acid site density, particle size and Si content. Ye et al. [23] have also studied the synthesis of SAPO-34 by hydrothermal method using different combinations of TEAOH and DEA as a template. In MTO conversion, the catalyst obtained using the concentration of 50% TEAOH and 50% DEA gave the longest lifetime due to optimal crystal size. Recently, Wang et al. [24] used triethyl amine (TEA) and TEAOH as mixture templates to synthesize SAPO-34. The outcomes indicated that the chemical composition, morphology, crystal size, and Si incorporation of SAPO-34 were affected greatly by the molar ratio of TEAOH/TEA.

Recently, combinations of different structure-directing agents have been employed during the synthesis of silicoaluminophosphates. This is because of economics, operational and technological views. For instance, the higher price of TEAOH leads to the problem in practical usage. Nevertheless, its superior catalytic performance encourages researchers to practice it as SDA. Furthermore, many researchers used morpholine as a template due to its ability to increase surface area and crystallinity [21, 25, 26]. However, written reports on the use of TEAOH/morpholine as the SDA in SAPO-34 synthesis are relatively immature. For each synthesized structure, there may exist an optimal templating agent or optimal combinations for a given mixed templating agent. The purpose of this paper is to investigate, exactly and systematically the effects of different combinations of Morpholine/TEAOH ratio on the morphology and the acidity of SAPO-34 and its performances on the catalytic test in MTO conversion.

2. Experimental

2.1. Catalyst

Crystalline SAPO-34 was synthesized hydrothermally using different combination of TEAOH and morpholine as the template. The source of Al, P and Si were aluminium isopropoxide (AIP, Merck), phosphoric acid (85 wt. % H_3PO_4, Merck), and Silicic acid (SiO_2, Merck), respectively. SAPO-34 was made by stirring and adding sequentially H_3PO_4, deionized water and aluminium source in a PE beaker. Then, the source of silicon was added in small amounts and after that the templates were applied. The gel molar composition was 1 Al_2O_3:1 P_2O_5: 0.4 SiO_2: X Morpholine, (2-X) TEAOH, 60 H_2O (X=0, 0.41, 1, 1.59, 2).The mixture was then placed in a 100 mL Teflon-lined stainless steel autoclave. The autoclave was placed in an oven at 463 K for

24 hours. The solid product was recovered, washed with distilled water and dried at 110 ^{o}C overnight. As-synthesized product was then calcined in air at 823 K for 6 h to remove the organic template and the water trapped within the micropores of solid.

2.2. Characterization

The X-ray diffraction (XRD) patterns of catalysts were obtained on a powder X-ray diffractometer (Bruker D8) using CuKa radiation (λ= 1.54 A°). For zeolite SAPO-34, the crystallinity was calculated as the ratio of the total area under the more important peaks at 2Θ ≈ 9.5^{o}, 13, 16 and 20.6[27]. The crystal size, morphology was analysed by scanning electron microscopy (SEM) using Philips XL30 microscopes, operating at 20 kV. Elemental analysis for Al, P and Si of calcined samples was done by inductively coupled plasma atomic emission spectrometry (ICP-AES) after dissolving the samples into 1 N nitric acid solution. The BET surface areas of calcined samples were determined from isotherm data of nitrogen adsorption–desorption using Micromeritics ASAP-2010 analyzer. Diffuse reflectance FTIR was conducted using a Bruker Tensor-27 spectrophotometer. The FTIR experiments of in-situ heat - treated samples were performed on pure powder of samples without KBr under flow of Nitrogen. IR spectra of the samples at the OH vibration region (3000–4000 cm^{-1}) were measured. The strength of acidity and acid site density of the catalysts was measured by temperature programmed desorption of ammonia (NH_3- TPD) using Micromeritics 2000. Prior to starting the tests, 0.2 g was pretreated at 300 °C under continuous flow of 30 ml min^{-1} helium and was subsequently cooled to the adsorption temperature of 100 °C. The temperature of the sample was then raised at a heating rate of 10 °C/min from 100 to 700 °C. The amount of ammonia desorbed from the catalyst was measured by comparing the TPD areas with those of the standard sample. ^{29}Si MAS NMR spectra were recorded at room temperature with a 4 mm probe scanning at 10

kHz. The internal standard for chemical shifts was 2, 2-dimethyl-2-silapentane-5-sulfonate sodium salt (DDS).

2.3. Catalyst Testing

The catalytic conversion of methanol to hydrocarbons was carried out in a fixed bed stainless steel reactor. The reactor consisted of a 45 cm long and 1.51cm outer diameter. The depth of the catalyst bed in the reactor was 5 cm. A detailed schematic diagram of the experimental set-up is shown in Fig.1. The catalyst was pretreated by heating it to 550 ^{o}C in a nitrogen flow (30mL min^{-1}). Methanol conversion to olefins was tested at 425 ^{o}C. The total pressure inside the reactor was approximately 1 bar for all of the experiments. During the reaction, bidistilled water was used as a diluent and co-fed with methanol into the reactor with a concentration of 70 wt. % in the feed. Catalyst weight (20-40 mesh pellet size) and the feed flow rate was set to obtain space time,$\tau = W / F^{0}_{MeOH}$, to 9 g_{cat}.hr/mol. The gas-phase components were analyzed online using a Hewlett-Packard 5890 flame ionization detector (FID) gas chromatograph (GC) equipped with Agilent J&W GS-alumina column and Plot column.

Figure1

3. Results and discussion

3.1 Characterization of the SAPO-34 catalysts

The X-ray diffraction patterns of synthesized catalysts prepared by different gel compositions are shown in figure 2. The powder XRD patterns of all the reported samples agree well with the previously reported pattern [27], except for minor changes in the relative X-ray peak intensities and positions. Furthermore, there is no additional peak of impurities in the samples. However, reflection intensity and crystallinity of products showed differently. The basis of comparison

among the crystallinity of samples is at four important locations, i.e.2Θ ≈ 9.5°, 13°, 15.9°, and 20.5°. Sample SP-2 presented the highest intensity of reflection. However, with increase of TEAOH ratio, a decrease in peak intensity and line broadening is observed. This observation indicated that a loss of crystallinity due to the higher TEAOH incorporation, which may lose the SAPO-34 phase.

When TEAOH is only applied as a template without using morpholine, the least intense reflection and a relatively ill-defined pattern is set up. This fact suggests that sample prepared with TEAOH could present crystal size significantly smaller than the remainder of the samples.

Based on the XRD peak intensities appearing at main locations, the crytallinity of SAPO-34 phase for sample SP-1 is higher than sample SP-0.41. The peaks appearing at 2Θ ≈ 9.5° and 20.6° for SP-0.41 are broader than those are for SP-1. This confirms the lower crystallinity of sample SP-0.41(X=0.41) compared to the SP-1 (X=1). The crystal size of both samples is the same, however, some roughness, kink and steps are found in the sample with lower crystallinity.

Figure 2

Figure 3 shows the SEM photos of the SAPO-34 catalysts. Despite their similar cubic-like rhombohedra crystalline shapes, their crystallite sizes and surface smoothness differed considerably. The approximate average crystal sizes of samples SP-0, SP-1.59 and SP-2 are sub-micrometer size (<1μm), 5μm and 7μm, respectively. The average sizes of samples SP-0.41 and SP-1 are the same (≈1 μm), however, some conflicts exist in the smoothness and defects. Low crystallinity occurs in the SEM images of samples as reduction in size and surface smoothness (roughness, kink, and steps) of crystallites. Sample SP-2 with the best crystalline has the largest crystals. The crystallinity loss of sample SP-1.59 relative to the sample SP-2 leads to a decrease in the size of former crystals. Although crystal size of sample SP-1 and SP-0.41 are the same, the

external surface of crystals of the latter one is more boisterous and has more number of kink and steps. Sample SP-0 had the smallest average particle size, which designates that the particle size has been lessened by an increment in the TEAOH contents in the gel mixture. These observations are consistent with XRD results discussed earlier, where crystallinity is observed to be diminished with increasing TEAOH ratio.

Figure3

Surface area and pore volume distributions of the samples calculated from the nitrogen adsorption-desorption isotherms are listed in Table 1. All the samples have surface area in the range 450-690 m^2/g. Sample SP-2 with the best crystalline has the maximum surface area. The variety of products crystallinity may happen with varying the involved TOT bond angle and length. Disorder development would affect the crystal growth in the crystal network. Generally, a reduction in the surface area was observed with increasing TEAOH. This notice is consistent with XRD results. A lower amount of surface area for SP-0 is highly associated to the low crystallinity and ill-defined pattern. Surface area of the sample SP-0.41 is higher than of that of SP-1 with the better crystallinity. It may be attributed to the higher external surface area for former sample.

Table1. Textural properties of samples after calcination

Sample	Surface area (m^2/g)			Pore volume (cm^3/g)		
	S_{micro}	S_{ext}	S_{total}	V_{micro}	V_{total}	V_{meso}
SP-0(X=0)	417	40	457	0.16	0.25	0.41
SP-0.41(X=0.41)	575	29	604	0.22	0.10	0.32
SP-1(X=1)	584	11	595	0.25	0.06	0.31
SP-1.59(X=1.59)	656	7	663	0.29	0.02	0.31
SP-2(X=2)	687	2	689	0.31	0.02	0.33

Sample SP-0, synthesized with pure TEAOH and having lowest surface area, presents higher value of pore volume (0.41 cm^3/g), non-microporous pore volume (0.25 cm^3/g) and external surface area (40 m^2/g). While, sample SP-2 has minimum non-microporous pore volume (0.02 cm^3/g) and external surface area (2 m^2/g).

The chemical composition of samples obtained by ICP-AES are presented in Table 2. In all the cases, the Si/ (Al + P) ratio of the samples is higher than that of the synthesis gels. This value is somewhat higher for samples synthesized with TEAOH. This implies that more amounts of Si were incorporated into the framework of SAPO molecular sieves. Furthermore, it remained as amorphous silica phase on extra framework. This can be confirmed with XRD patterns, which expressed an increase in crystallinity with lower amount of Si content.

Table2. Elemental composition (molar basis)

Sample	Molar composition of gel	$Si/(Al + P)_{gel}$	$Si/(Al + P)_{Solid}$	Si incorporation
SP-0.00	$Si_{0.09}Al_{0.455}P_{0.455}O_2$	0.10	0.16	1.37
SP-0.41	$Si_{0.09}Al_{0.455}P_{0.455}O_2$	0.10	0.13	1.26
SP-1.00	$Si_{0.09}Al_{0.455}P_{0.455}O_2$	0.10	0.12	1.21
SP-1.59	$Si_{0.09}Al_{0.455}P_{0.455}O_2$	0.10	0.11	1.13
SP-2.00	$Si_{0.09}Al_{0.455}P_{0.455}O_2$	0.10	0.11	1.12

Acidity plays an significant function in the catalytic properties of solid acid catalysts. TPD profile of ammonia desorption from prepared pure SAPO-34 samples is shown in Figure 4. Two TPD peaks for SAPO-34 samples, centered around 180–210 and 440–460 °C as low and high temperature desorption sites were observed.

The first desorption peak of TPD curves was attributed to the hydroxyl groups (OH) bounded to the defect sites, i.e. POH, SiOH, and AlOH. The larger area of first desorption peak, the more defect sites would be associated with the sample. The area under the first desorption peak

increases in the following sequences: SP-0> SP-0.41> SP-1> SP-1.59> SP-2. TPD results were in good agreement with the XRD patterns. These sites have little effect on the MTO performance of SAPO-34 samples, because ammonia molecules desorbs before 300 ^{o}C from these sites. Therefore, methanol as a weak basic molecule cannot be converted to light olefins at a reaction temperature of above 400 ^{o}C on these sites.

The second desorption peak was set apart to the bridging hydroxyl group as a strong Bronsted acid site[28]. These hydroxyl groups are responsible for the catalytic process at high temperatures. The concentration of bridging hydroxyl group varies with TEAOH/morpholine ratio in the initial gel. It should be mentioned that the higher desorption temperature represents the stronger acid sites. From TPD, the acid sites of samples with more TEAOH are stronger than those with morpholine. This is due to the more silicon environment into the framework via substitution mechanism 3(SM3), in which the incorporation of Si takes place via a simultaneous substitution of a pair of adjacent Al and P atoms by two Si atoms. This observation is in accord with the results of in-situ FTIR spectra in the OH stretching region and ^{29}Si MAS NMR spectra of SAPO-34 samples.

Figure4

TPD results were in good agreement with the results of in situ FTIR spectra of samples at the OH vibration region (Fig.5). Two bands appearing at 3603 and 3587 cm^{-1} in the spectra of SAPO-34 samples can be attributed to the hydroxyl group of the Bronsted acid sites and located inside the double six rings.

Figure5

There is a difference in the concentration of the strong acidic hydroxyl groups. Sample SP-2 indicates the presence of a higher amount of Bronsted acid sites. The fact that the two IR bands at 3603 and 3587 cm^{-1} are much weaker for SP-0 than other samples indicates the presence of a lower amount of Bronsted acid sites in this sample. A band appearing at 3665 cm^{-1} is assignable to defect site on the external surface of SAPO-34 crystallite [29, 30]. This band is weaker for SP-1 than the sample SP-0.41, indicating more defect sites in the latter sample. This observation is likewise confirmed by XRD data in Fig.1, where showed a line broadening in XRD peak for SP-0.41.

^{29}Si MAS NMR was performed to examine the Si environment into the SAPO-34 framework (Fig.6). According to the literature[21], the peaks at δ=-92.5, -96.5, -101, -106, -111 are attributed to Si(4Al), Si(3Al), Si(2Al), Si(1Al), and Si(0Al) environments, respectively.

Figure6

In the ^{29}Si MAS NMR spectra, the incorporation of isolated Si atoms generates SiOHAl groups with strong-acid properties. This also approves the Si directly incorporation in the crystallization or the SM2 substitution mechanism. The NMR spectra of sample SP-2 indicates that most of its silicon atoms are in phosphorous positions, thereby leading Si surrounded by 4 Al atoms in the second coordination shell (mechanism SM2). This is in good agreement with FT-IR spectra.

The proportion of Si(4Al) environments decreases with increasing TEAOH content in the initial gel. Meanwhile, the proportions of the other Si environments increase. The samples with lower crystallinity possess a multiple silicon environment. The heterogeneous coordination state of the sample SP-0 may have been made by its extremely small crystallite size. The resulting large external surface area generated insufficient numbers of coordination sites, thereby inducing the broad shoulder of the ^{29}Si MAS NMR peaks. It is shown that template can affect the Si

distribution in SAPO-34. It should be noted that a higher number of acid sites are brought forth through the SM2 mechanism, while substitution via SM2 + SM3 results less but stronger acid sites. This suggestion was confirmed by the NH_3- TPD profiles.

3.2 Catalytic test

The catalytic activity of these materials in the MTO reaction was studied at a temperature of 425 ^oC and space time of 9 $g_{cat}.hr/mol$. Figure 7 shows the yield of ethylene, propylene, butene and total olefins with various M or process times for 5 catalysts. M is defined as the total weight of methanol fed to the reactor during the run per unit weight of catalyst. The yield of ethylene increased gradually with process time. The yield of propylene and butene shows slightly decreases during the reaction. One cause of increasing the ethylene selectivity is therefore from the decreases in selectivities to propylene and butene. These products are more active than ethylene. They can undergo oligomerization more easily to form bigger oligomers that would be entrapped in the cages of SAPO-34. The ethylene to propylene ratio reached to a maximum before breakthrough point. This point depends on the amount of catalyst, the water content of the feed and the morphology of as-synthesized material.

The main problem of SAPO-34 with the MTO process is the rapid deactivation attributed to the deposition of high molecular weight hydrocarbons on the pore entrance[19]. In this study, sample SP-1 synthesized with a TEAOH / morpholine ratio of 1:1 exhibited an improved stability in this reaction. The sample SP-2 shows the shortest lifetime. This may be attributed to the low external surface area and crystal size. Big crystal has a long intracrystalline diffusion path enough for the reaction intermediates to react into coke. Furthermore, the strong acidity of SP-2 catalyst promoted hydrogen transfer reaction of olefin to saturated hydrocarbons and aromatic and

thereby successive polymerization easily occurs. Smaller crystal size enhances the lifetime of catalyst by reducing the possibility of reentering the ethylene and propylene. Therefore, the adsorption of the products into the SAPO-34 must be lowered. The comparison between samples SP-0, SP-0.41 and SP-1 reveals that local disorders could lead to the expansion of the space of channels or cages around the defect sites. This steps up the framework blockage due to formation of large hydrocarbon molecules during MTO reaction. This phenomenon decreases the overall rate of diffusion of the MTO products in the crystal size [29]. Therefore, among the samples with approximately equal crystal size, sample SP-1 with better crystallinity maintains longer the main product yield. It should be noted that small crystallites are favorable for catalysis due to large exposed external surfaces and short diffusion paths. Nevertheless, extremely small SAPO-34 and very low crystallinity can reduce catalytic activity. The large external surfaces of the very small crystallites lead to reduced inner surface areas, thereby lowering the number of acid sites in the micropores that act as active sites [30].

Figure7

As shown in Fig. 7, all samples have similar high selectivity to light olefins, the most striking feature is the difference in the catalyst lifetime. The product distribution and selectivity variation in a sample depend highly on the operating condition, such as temperature, space velocity and the water content feed. However, the lifetime of catalyst depends highly on the crystal size and morphology of the sample. Sample SP-1 exhibited the longest lifetime. The lifetime was in the order of SP-1> SP-0.41> SP-0> SP-1.59 > SP-2. The combination of high external surface area and small crystal size and better crystallinity, facilitating the accessibility of the reactant molecules to the acid sites and optimum acidity could be the reasons to explain the better catalytic performance of catalyst SP-1.

Fig. 8 displays the product yields During MTO reaction at 425 ^{o}C and 9 g_{cat}.h/gmol process time over five different SAPO-34 catalysts after 120 min on stream (M ≈ 7). Generally, a substantial increase in methane product and a simultaneous decrease in the amount of light alkenes were found. With time on stream, methane formation is related to the deactivation process. Methane yield over SP-2 after 2 h on stream was significant because of its rapid deactivation. Deactivation and methane formation are essential features with respect to the reaction mechanism and the contribution of diffusional constrains in the narrow pore structure [11, 31]. With time on stream, more bulky hydrocarbons are formed in the acidic center of catalyst. As these molecules cannot be desorbed because of diffusional hindrance, they act as hydrogen donors for the transformation of the methoxy groups to methane. Sample SP-1 with the mild acidity and small crystal size did not make as much methane as the other samples.

Figure8

4. Conclusions

SAPO-34 molecular sieves synthesized with different combination of TEAOH and morpholine as structure directing agents are proven to exhibit different physicochemical properties, especially textural parameters and particle size. It is demonstared that the nature of the template used in the synthesis affects the morphology of the final crystal due to the different rate of crystal growth. All the prepared SAPO-34 catalysts showed approximately similar activity and product distribution in the MTO reaction. However, the catalyst produced by the TEAOH/morpholine ratio of 1:1 showed the longest lifetime due to optimal crystal size and acidity. The outcomes established that on chabazite catalyst, methane selectivity increased when light olefins decreased due to coke deposits.

Nomenclature:

C	mole ratio of morpholine to alumina
M	total weight of methanol during the run per unit weight of catalyst ($process\ time$)
MW	molecular weight
T	temperature
TEAOH	tetraethylammonium hydroxide
SP	sample
XRD	X − ray diffraction
FTIR	fourier transform infrared spectroscopy
BET	brunauer, emmett and teller
SEM	scanning electron microscope
ICP	Inductively coupled plasma

REFERENCES

[1] M. Sedighi, M. Ghasemi,M. Mohammadi and S. H. A. Hassan, A novel application of a neuro–fuzzy computational technique in modeling of thermal cracking of heavy feedstock to light olefin, RSC Adv.,2014, 4, 28390-28399.
[2] M. Sedighi, K. Keyvanloo, J. Towfighi, Experimental study and optimization of heavy liquid hydrocarbon thermal cracking to light olefins by response surface methodology, Korean Journal of Chemical Engineering., 2010, 27, 1170-1176.
[3] M. Sedighi, K. Keyvanloo, J. Towfighi, Modeling of thermal cracking of heavy liquid hydrocarbon: application of kinetic modeling, artificial neural network, and neuro-fuzzy models, Industrial & Engineering Chemistry Research., 2011,50, 1536-1547.
[4] A. Xing, L. Wang, Y. Shi, Evolution of Coke Deposit and Its Effect on Product Selectivity for Methanol-to-Olefin Reaction in Fixed Fluidized bed, Energy & Fuels., 2014, 28, 3339-3344.
[5] M. Bjørgen, S. Svelle, F. Joensen, J. Nerlov, S. Kolboe, F. Bonino, L. Palumbo, S. Bordiga, U. Olsbye, Conversion of methanol to hydrocarbons over zeolite H-ZSM-5: On the origin of the olefinic species, Journal of Catalysis., 2007, 249, 195-207.
[6] C.D. Chang, J.C. Kuo, W.H. Lang, S.M. Jacob, J.J. Wise, A.J. Silvestri, Process studies on the conversion of methanol to gasoline, Industrial & Engineering Chemistry Process Design and Development., 1978, 17, 255-260.
[7] A.G. Gayubo, A.T. Aguayo, M. Olazar, R. Vivanco, J. Bilbao, Kinetics of the irreversible deactivation of the HZSM-5 catalyst in the MTO process, Chemical engineering science., 2003, 58, 5239-5249.
[8] J. W. Park, J. Y. Lee, K. S. Kim, S. B. Hong, G. S, Effects of cage shape and size of 8-membered ring molecular sieves on their deactivation in methanol-to-olefin (MTO) reactions, Applied Catalysis A: General.,2008, 339, 36–44.
[9] Guozhen Qi, Zaiku Xie, Weimin Yang, Siqing Zhong, Hongxing Liu, Chengfang Zhang, Qingling Chen, Behaviors of coke deposition on SAPO-34 catalyst during methanol conversion to light olefins, Fuel Processing Technology., 2007, 88, 437–441

[10] Arvind Kumar Singh, Rekha Yadav, Vasanthakumaran Sudarsan, Kondamudi Kishore, Sreedevi Upadhyayula and Ayyamperumal Sakthivel , Mesoporous SAPO-5 (MESO-SAPO-5): a potential catalyst for hydroisomerisation of 1-octene, *RSC Adv.*, 2014,**4**, 8727-8734.

[11] M. Popova, C. Minchev, V. Kanazirev, Methanol conversion to light alkenes over SAPO-34 molecular sieves synthesized using various sources of silicon and aluminium, Applied Catalysis A: General .,1998, 169, 227-235.

[12] G. LIU, P. TIAN, Z. LIU, Synthesis of SAPO-34 molecular sieves templated with diethylamine and their properties compared with other templates, Chinese Journal of Catalysis., 2012, 33, 174-182.

[13] M. Sedighi, J. Towfighi, A. Mohamadalizadeh, Effect of phosphorus and water contents on physico-chemical properties of SAPO-34 molecular sieve, Powder Technology., 2014, 259, 81-86.

[14] A. Izadbakhsh, F. Farhadi, F. Khorasheh, S. Sahebdelfar, M. Asadi, Y.Z. Feng, Effect of SAPO-34's composition on its physico-chemical properties and deactivation in MTO process, Applied Catalysis A: General., 2009, 364, 48-56.

[15] A. Izadbakhsh, F. Farhadi, F. Khorasheh, S. Sahebdelfar, M. Asadi, Z. Yan, Key parameters in hydrothermal synthesis and characterization of low silicon content SAPO-34 molecular sieve, Microporous and Mesoporous Materials., 2009, 126, 1-7.

[16] Yasuyoshi Iwase, Ken Motokura, To-ru Koyama, Akimitsu Miyaji and Toshihide Baba , Influence of Si distribution in framework of SAPO-34 and its particle size on propylene selectivity and production ratefor conversion of ethylene to propylene, *Phys. Chem. Chem. Phys.*, 2009,11, 9268-9277

[17] Zhibin Li, Joaquín Martínez-Triguero, Patricia Concepción, Jihong Yu and Avelino Corma , Methanol to olefins: activity and stability of nanosized SAPO-34 molecular sieves and control of selectivity by silicon distribution, *Phys. Chem. Chem. Phys.*, 2013,15, 14670-14680.

[18] B.M. Lok, C.A. Messina, R.L. Patton, R.T. Gajek, T.R. Cannan, E.M. Flanigen, Silicoaluminophosphate molecular sieves: another new class of microporous crystalline inorganic solids, Journal of the American Chemical Society.,1984, 106, 6092-6093.

[19] Jérémy Faye, Atsushi Takahashi, Mickaël Capron, Pascal Fongarland, Franck Dumeignil and Tadahiro Fujitani , Al-modified mesoporous silica for efficient conversion of methanol to dimethyl ether, *RSC Adv.*, 2013,**3**, 5895-5902.

[20] Q. Wang, L. Wang, H. Wang, Z. Li, H. Wu, G. Li, X. Zhang, S. Zhang, Synthesis, characterization and catalytic performance of SAPO-34 molecular sieves for methanol-to-olefin (MTO) reaction, Asia-Pacific Journal of Chemical Engineering .,2011, 6, 596-605.

[21] T. Álvaro-Muñoz, C. Márquez-Álvarez, E. Sastre, Use of different templates on SAPO-34 synthesis: Effect on the acidity and catalytic activity in the MTO reaction, Catalysis Today.,2012, 179, 27-34.

[22] S. Wilson, P. Barger, The characteristics of SAPO-34 which influence the conversion of methanol to light olefins, Microporous and Mesoporous Materials .,1999, 29 117-126.

[23] L. Ye, F. Cao, W. Ying, D. Fang, Q. Sun, Effect of different TEAOH/DEA combinations on SAPO-34's synthesis and catalytic performance, Journal of Porous Materials.,2011, 18 225-232.

[24] P. Wang, A. Lv, J. Hu, J.a. Xu, G. Lu, The synthesis of SAPO-34 with mixed template and its catalytic performance for methanol to olefins reaction, Microporous and Mesoporous Materials.,2012, 152 178-184.

[25] R. B. Rostami, M. Ghavipour, R. Behbahani, A. Aghajafari, Improvement of SAPO-34 performance in MTO reaction by utilizing mixed-template catalyst synthesis method, *J. Nat. Gas Science and Eng.,2014, 20, 312-318*

[26] N. Fatourehchi, M. Sohrabi, S. J. Royaee, S. Mahdi MirarefinPreparation of SAPO-34 catalyst and presentation of a kinetic model for methanol to olefin process (MTO), Chemical Engineering Research and Design, 2011, 89, 811–816

[27] B. Lok, T.R. Cannan, C. Messina, The role of organic molecules in molecular sieve synthesis, Zeolites .,1983, 3282-291.
[28] Z. Zhu, M. Hartmann, L. Kevan, Catalytic Conversion of Methanol to Olefins on SAPO-n (n= 11, 34, and 35), CrAPSO-n, and Cr-SAPO-n Molecular Sieves, Chemistry of materials.,2000, 12, 2781-2787.
[29] K. Hemelsoet, A. Ghysels, D. Mores, K. De Wispelaere, V. Van Speybroeck, B.M. Weckhuysen, M. Waroquier, Experimental and theoretical IR study of methanol and ethanol conversion over H-SAPO-34, Catalysis today.,2011, 177, 12-24.
[30] H.-G. Jang, H.-K. Min, J.K. Lee, S.B. Hong, G. Seo, SAPO-34 and ZSM-5 nanocrystals' size effects on their catalysis of methanol-to-olefin reactions, Applied Catalysis A: General .,2012, 437, 120-130.

[31] F. Salehirad, M.W. Anderson, Solid-State^{13}C MAS NMR Study of Methanol-to-Hydrocarbon Chemistry over H-SAPO-34, J. Catal. ,1996, 164, 301.

List of figures

Figure7. Yields of ethylene, propylene, butene and C_2-C_4 olefins with run length over SAPO-34 catalysts. (a)X=0, (b) X=0.41, (c) X=1, (d) X=1.59, (e) X=2. Feed: 30 wt.% methanol with 70 wt.% water, Temperature: 425 °C, $W/F^0_{MeOH} = 9\ g_{cat}.hr/mol.$

Figure8. Yields of methane and total olefins During MTO reaction over five different SAPO-34 catalysts after 120 min on stream

List of tables

Table1. Textural properties of samples after calcination
Table2. Elemental composition (molar basis)